Tectonophysics 661 (2015) 200–209

Contents lists available at ScienceDirect

Tectonophysics

journal homepage: www.elsevier.com/locate/tecto

Late Quaternary evolution of the La Cantera Fault System (Central Precordillera, Argentina): A morphotectonic and paleoseismic analysis

Laura Perucca [a,b,*], Martín Rothis [a,b], Francisco Hilario Bezerra [c,d], Nicolás Vargas [a], Jean Lima [d]

[a] Departamento Geología, Facultad de Ciencias Exactas, Físicas y Naturales — Universidd Nacional de San Juan, Av. Ignacio de La Roza y Meglioli, 5400 San Juan, Argentina
[b] CONICET, Gabinete de Neotectónica y Geomorfología, INGEO-CIGEOBIO — Facultad de Ciencias Exactas, Físicas y Naturales — Universidd Nacional de San Juan, Av. Ignacio de La Roza y Meglioli, 5400 San Juan, Argentina
[c] Departamento de Geologia, Universidade Federal do Rio Grande do Norte, Campus Universitario, Natal, RN 59068-570-UFRN, Brazil
[d] Programa de Pós-Graduação em Geodinâmica e Geofisica, Campus Universitario, Natal, RN 59068-570-UFRN, UFRN, Brazil

ARTICLE INFO

Article history:
Received 24 April 2015
Received in revised form 15 August 2015
Accepted 21 August 2015
Available online 12 September 2015

Keywords:
Neotectonics
Thrust
Paleoseismicity
Holocene
Central Precordillera

ABSTRACT

The La Cantera Fault System (LCFS) is the most active Quaternary structure in the Central Precordillera of San Juan, in central-western Argentina; the system extends for 47 km along the intermountain valley that separates the Sierra de La Cantera and La Invernada, north of the San Juan River. The average fault trend is 20°; it dips at angles varying between 15° and 30° W in the northern section, to approximately 40° W in the central section, and up to 60° W in the southern section. The fault affects Holocene to recent alluvium deposits in the western piedmont of the Sierra de La Cantera and is defined by a series of landforms found in compressive tectonic environments, including simple and compound counterslope fault scarps, staircased alluvial terraces, sag ponds, flexural scarps, aligned springs, broom-shaped drainage patterns, river diversions, beheaded channels, changes in incision depths, sinuosity and a river gradient along channels. Trench investigations indicated that at least three events occurred in the past 1.1–10.1 ky. The topographic profiles of the selected channels and interfluves cutting across the northern and central trace of the fault were analyzed using a Stonex Vector GPS differential system to establish the relationship between the topography and slope of the rivers. This morphometric analysis of scarps indicates that active tectonics have played an essential role in controlling the drainage pattern in the piedmont, leading the rivers to adjust to these slope variations. Based on the analyzed geomorphologic, stratigraphic and structural characteristics, the LCFS is considered to be a relevant seismogenic source in the intraplate portion of southern South America, with a recurrence interval of at least 2000 ± 500 years for moderate magnitude earthquakes during the last 11,000 years.

1. Introduction

The Andean Precordillera of western Argentina is a first-order morphotectonic unit of the Pampean Segment of the flat subduction between 27° S and 33° S, being one of the most seismically active zones of thrust tectonics in the world. This area has more than 90% of the Quaternary deformation documented in Argentina (Costa et al., 2006), where crustal seismicity is characterized by high levels of earthquake activity with hypocentral depths ranging from 5 to 35 km (Smalley and Isacks, 1990; Smalley et al., 1993). Nevertheless, there are no clear relationships between main Quaternary deformations and these seismic events.

Up to now, papers describing Quaternary deformations in this portion of Central Precordillera are very scarce. For example, Whitney and Bastías (1984) described several features with Quaternary tectonic activity in the western piedmont of the Sierra de La Cantera. More recently, Mingorance (1998) analyzed two sections along the fault trace and identified that at least three individual seismotectonic events of varying magnitudes and located along the La Cantera fault were generated by the fault in prehistoric and historic times. Millán and Perucca (2011) also carried out a brief analysis of natural trenches and drainage anomalies located in the northern section of the fault section and Perucca et al. (2014a,b) described the morphotectonic and neotectonic controls on river pattern along Sierra de la Cantera piedmont. This fault system, however, lacked fault chronology associated with accurate topography that could constrain its geodynamic significance. In addition, more field-based studies are necessary to address the problems of fault recurrence and the chronology and magnitude of paleoseismic events along Quaternary-active faults in the region.

The purpose of this work is to analyze and date Late Quaternary tectonic activity along the La Cantera Fault System (LCFS), especially in its central and northern sections and address the relationship between this fault system and the regional deformation and neotectonic setting for a

* Corresponding author at: Departamento Geología, Facultad de Ciencias Exactas, Físicas y Naturales — Universidd Nacional de San Juan, Av. Ignacio de La Roza y Meglioli, 5400 San Juan, Argentina.
E-mail address: lperucca@unsj-cuim.edu.ar (L. Perucca).

http://dx.doi.org/10.1016/j.tecto.2015.08.041
0040-1951/

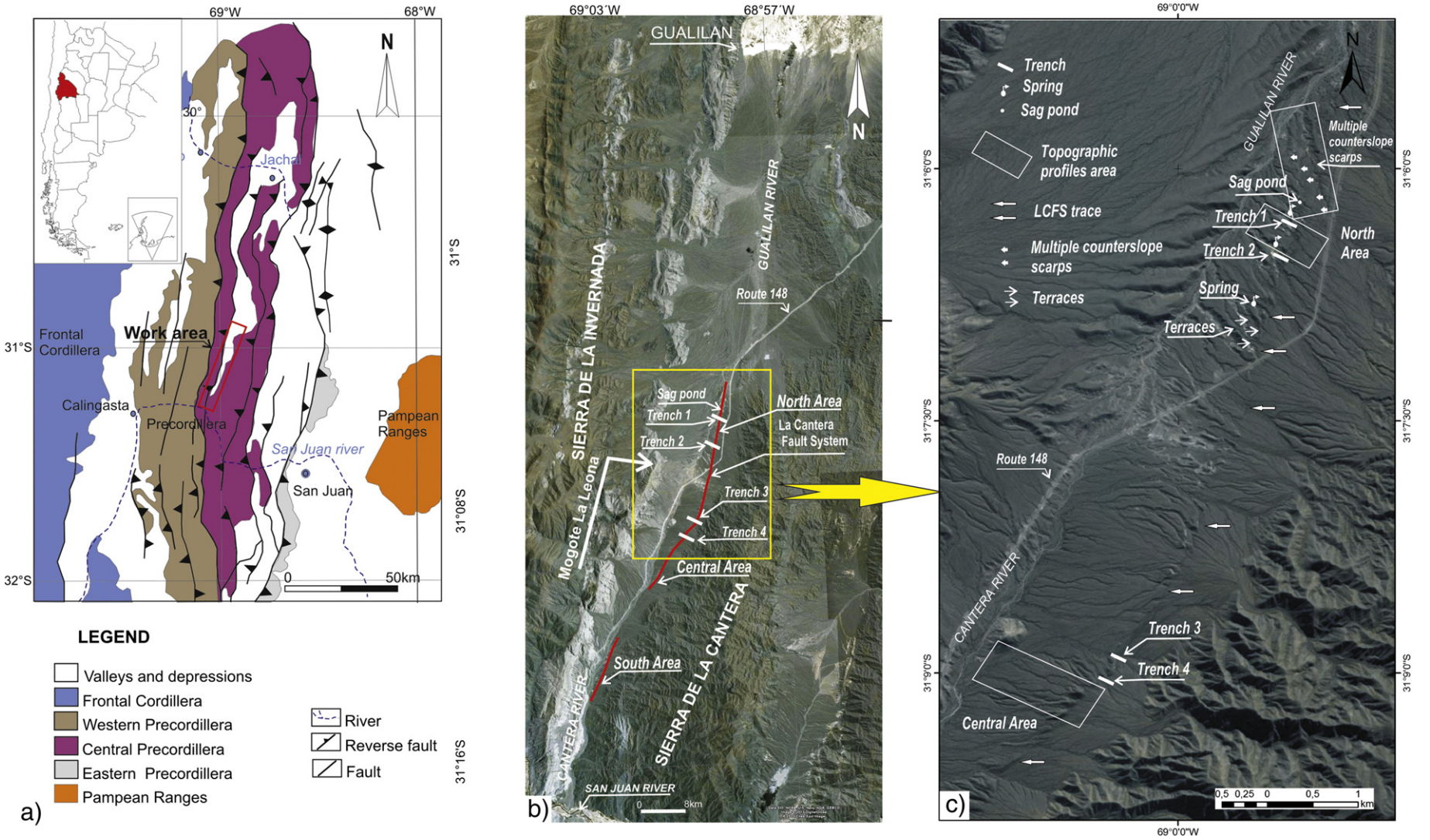

Fig. 1. a) Geological sketch map of central-western Argentina, from 30° to 32° SL (modified from Ramos and Vujovich, 2000); b) Google Earth image, on which natural exposures or trench locations along the LCFS are reported, yellow rectangle shows location of c. c) Detailed Google Earth image showing main fault trace, on which natural exposures, topographic profiles areas and geomorphic features like multiple counterslope scarps, unpaired terraces, springs and sag ponds are indicated.

better understanding of the neotectonic evolution of this portion of the Central Andean thrust. The study area is located in a tectonic valley between Sierra de La Invernada and La Cantera in the Central Precordillera geological province (31° 04′–31° 10′S and 69° 01′–68° 58′W), northwest of San Juan, Argentina (Fig. 1a). The Sierra de La Invernada is a mountain chain that trends north–south, with a maximum height of 3700 m asl. The Sierra de La Cantera also has a north–south trend and a height of 3100 m asl.

In the western piedmont of the Sierra de La Cantera, rock outcrops corresponding to the lower and middle members of the Pachaco Formation (Uppermost Oligocene–Miocene) are exposed (Levina et al., 2014). The Neogene strata have a westward-dipping homoclinal arrangement and trend north–south. The dip of the strata ranges from 21° W in the eastern portion to approximately 50° near the fault zone. The Quaternary deposits correspond to alluvial fans that are affected by the La Cantera fault, as well as river terraces, colluvial fans and debris cones on the slopes of the mountain fronts. Rivers and streams located on the eastern foothills of the Sierra de La Invernada and the western piedmont of the Sierra de La Cantera drain from Mogote La Leona hills north to Pampa de Gualilán, by the Gualilán River (Fig. 1b). South of the Mogote La Leona, streams from both the Sierra de La Invernada and Sierra de La Cantera drain to the south through the La Cantera gorge to the San Juan River (Fig. 1b).

The western piedmont of the Sierra de La Cantera has an average width of 1.64 km, decreasing to only 400 m in the south at the La Cantera River mouth in the San Juan River. In this piedmont, alluvial fans with evidence of active faulting associated with the La Cantera Fault System (LCFS), are the dominant landform (Fig. 1b, c). The morphotectonic expression of this system includes subparallel Quaternary-active faults, simple and compound counterslope fault scarps, strath and fill terraces, flexural scarps, progressive unconformities, alluvial Quaternary folding and anomalous drainages (Perucca et al., 2014a,b). The fault scarp height varies along the fault between 0.30 m and 13.0 m, representing the highest elevations in the central section. The morphotectonic evidence in the Quaternary deposits is more evident and increase from south to north of the fault, where the latest evidence of the Holocene and potential historic activity was found.

2. Tectonic setting

2.1. General tectonic features of the Precordillera region

Between 29° and 33° S, with a convergence azimuth of approximately 78° (Vigny et al., 2009), the Nazca plate is being subducted at a rate of 6.3 cm/year beneath the South American plate to depths up to 100 km (Barazangi and Isacks, 1976; Kendrick et al., 2003; Pardo-Casas and Molnar, 1987; Yáñez et al., 2001).

The flat geometry of the subducted slab can be attributed to the oblique subduction of the Juan Fernández ridge underneath the South American plate (Martinod et al., 2010; Pilger, 1981; Rosenbaum and Mo, 2011). In this area, Late Miocene–Quaternary tectonics has resulted in the development of the Frontal Cordillera, Precordillera and the Pampean Ranges in the eastern foreland of San Juan (Ramos, 1988, 1999; Ramos et al., 2002).

The Central Precordillera comprises mountain ranges extending from 29° to 32° S latitudes. It has been described by several authors (Allmendinger et al., 1990; Cristallini and Ramos, 2000; Jordan et al., 1993; von Gosen, 1992) as a characteristic thin-skinned, thrust-and-fold belt resulting from Neogene crustal shortening on western dipping, imbricated structures that root down to a 10–15 km deep main *décollement*. In this region, most of the active structures are related to compressional faulting (Siame et al., 2006). However, earthquakes on these active reverse faults are not always accompanied by surface ruptures.

A series of geologic and tectonic factors are occurring where the Nazca Plate is subducting sub-horizontally, between 29° and 33° S and substantial part of the Quaternary deformations in Argentina is concentrated in this region (Costa et al., 2006). Here, the main seismogenic sources can be located and defined with certitude. Such sources show different degrees of activity. Generally, they are sub-parallel faults, predominantly N–S trending. It is precisely in this intraplate setting that the most important destructive earthquakes take place. They were related to surface ruptures, such as the earthquakes of 1894 (M 7.5), 1944 (Mw 7.0) and 1977 (Mw 7.4) (Alvarado and Beck, 2006), all of them occurred between these latitudes (Perucca et al., 2006). On the other hand, the last historic event that occurred in the northern portion of LCFS was the 1924 earthquake (Ms = 6.0) (Mingorance, 1998). However, there is no evidence of surface rupture for this event, behaving the structure like a blind thrust.

2.2. Local geology of La Cantera Fault System

The geology of the area is characterized by fine and coarse sandstones to fine conglomerates of the Pachaco Formation from the Oligocene to Late Miocene age (Levina et al., 2014; Milana et al., 1993) that outcrops into the western piedmont of the Sierra de La Cantera and is commonly associated with the fault system. The sandstone delineates a westward-dipping homoclinal structure that was produced by reverse faulting of the west-dipping La Cantera active fault. Neogene rocks are covered by Quaternary alluvial deposits composed of coarse-grained loose sandy-gravel layers with an average total thickness of approximately 1–3 m. The regional structure consists of an east-verging imbricated fan comprised of an array of separated to overlapping fault-propagation folds and out-of-sequence structures (Ramos et al., 1997). Morley (1988) pointed that out-of-sequence faults show hinterland propagation and are caused by the development of new thrust faults through a deformed thrust sheet. According to von Gosen (1992), younger faults formed in front of the stack of imbricates, whereas the earlier-formed imbricates continued their movements along the preexisting thrust faults, which were steepened or overturned.

LCFS is an out-of-sequence fault (Cristallini, 1998), where the uppermost part of the Ordovician carbonates (San Juan Formation) form the base of the imbricate sequence. This is imaged in the central section of the fault system at two outcrops where Ordovician limestones thrust onto Neogene deposits and Quaternary alluvial levels (Fig. 2a). Although the fault planes are not clear, calcareous megaboulders along the fault trace and fault breccias with calcareous cement and very angular limestone clasts, ranging from 1 cm to 70 cm, were observed in the counterslope scarp (Fig. 2b–d). However, on surface, this fault zone primarily affects Neogene and Quaternary formations.

The geometry of the mountain ranges and the kinematics of the LCFS exhibit an almost W–E oriented compression responsible for the current processes of relief formation, which corresponds to the direction of the vector of deformations associated with the Nazca-South America collision proposed by Pardo et al. (2002) and Anderson et al. (2007), among others.

3. Data and methods

Because of the great sensitivity of alluvial rivers to variations of the topographic gradient we carried out a morphotectonic analysis of the alluvial fans and rivers that cross the LCFS. High resolution elevation sections were performed in order to highlight the topography of the terrain and document the Holocene tectonic evolution of the area.

As was pointed by Perucca et al. (2014a) in the northern portion of the LCFS, counterslope scarps affect the river courses of a piedmont modifying their courses according to the meso and micro-topographic changes due to the differential uplift-subsidence patterns. In this way, under certain conditions, rivers tend to evolve, increasing their sinuosity or modifying their pattern and flow direction (Holbrook and

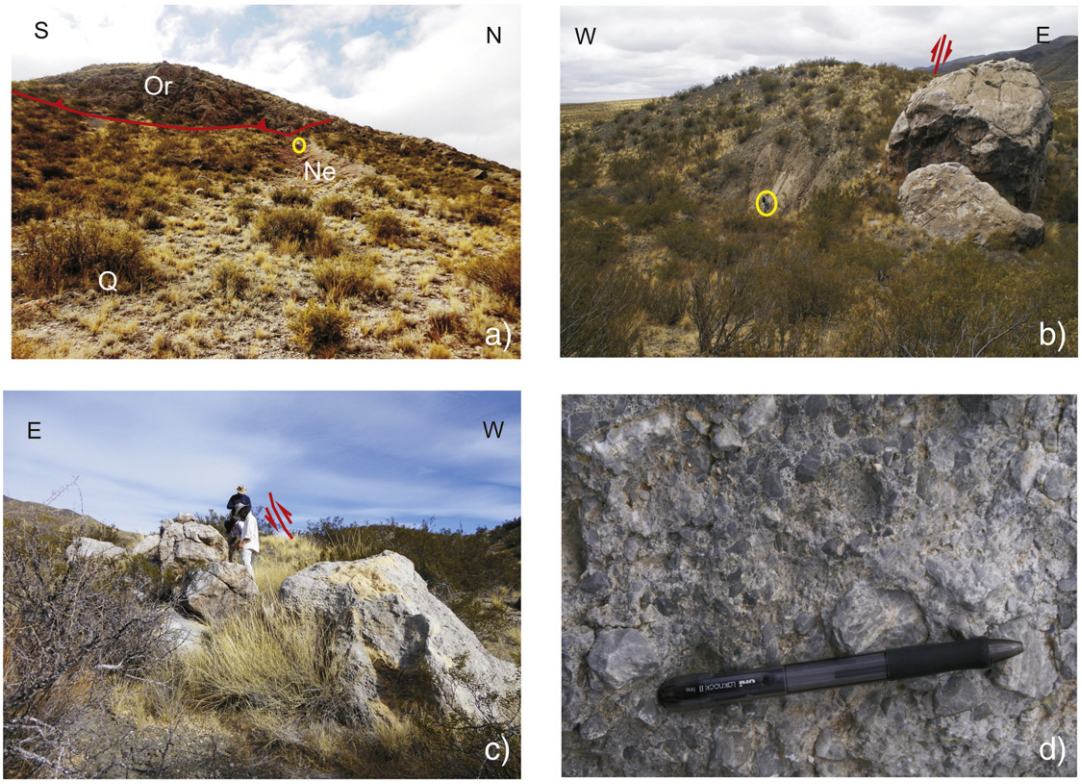

Fig. 2. a) Ordovician limestones thrust over the Neogene succession forming the base of east-verging thrusts. Yellow circle: person is for scale; b) highest counterslope scarp with limestone megaboulders, c) calcareous brecciated boulders along the fault trace; c) Detail of limestone breccia found in the contact area between the fault blocks.

Schumm, 1999). In this study, we analyzed several rivers and their interfluves in the northern and central portion of LCFS as this behavior is influenced by tectonic movements.

Detailed fault scarp data were acquired using a differential GPS by measuring high-resolution topographic profiles perpendicular to the LCFS scarps (named in this work as North and Central sections) (Fig. 3a, b). In the north section, seven NW–SE and W–E profiles were carried out, from which three were surveyed along rivers and four in the interfluves. To highlight the topography of the terrain through detailed high-resolution elevation sections, the profiles were selected using easy-access sections to improve coverage with the measurement devices. A detailed photo-interpretation of the area allowed for the final selection of several transects perpendicular to the fault scarps, and longitudinal profiles along the rivers that cross the faults to highlight particular morphological patterns, like scarp heights, changes in the gradient of the alluvial fans, anomalous slopes, which could be related to the Quaternary tectonic activity of faults. The topographic profiles were carried out with a GPS differential system, with a high performance GPS/SBASS L1 receiver that also has EVEREST signal filtering technology. The measurements were obtained using the following parameters: positioning and configuration of each device in manual mode, selection of a record at 2-second intervals, a mask angle of 10 and track times of 2 s. For the field data collection, one of the devices was stationed at one point and the other was used as a rover. Processing the field data involved correction, using software provided by the differential GPS system. The data from the high resolution elevation profiles perpendicular to the fault scarp (North and Central sections; Fig. 3) were also applied to determine the slope changes in each transect.

Four natural exposures, located in river channels of the North and Central section of the LCFS, were analyzed and dated to know the kinematics of the fault and the age and characteristics of the alluvial levels affected by faults (Fig. 1b). All of the samples were analyzed using an Accelerator Mass Spectrometry (AMS) method at Beta Analytic. All of the results that fell within the range of available calibration data were calibrated to the calendar years (cal BC/AD) and calibrated to the radiocarbon years (cal BP). Calibration was performed using one of the databases associated with the 2013 INTCAL program.

4. Results

4.1. Tectonic topography of the LCFS

As McCalpin (2009) already pointed out, topographic profiling is often the easiest method of documenting the vertical component of paleoseismic faulting. These profiles recorded across fault scarps and along rivers running through the fault trace provide a measurement of vertical surface offset, which is related to fault displacement and stream anomalies. So, we measured several topographic profiles across the fault trace in order to characterize scarp morphology and help constrain fault behavior.

The slope average obtained in the topographic profiles of the mid and distal sections of the Western piedmont of the Sierra de La Cantera is between 5° and 8°. This result partially encompasses alluvial fans slopes values that were measured under normal conditions, which varied from 12° to 2° from the apex to the distal section (Gutiérrez Elorza, 2008). However, these could be considered high slope values for distal sections.

In the North portion (Fig. 3a), the topographic height of the interfluve profiles decreases towards WNW. The topographic profiles of the interfluves exhibit disruptions, such as small bulges with an asymmetric shape, which caused a steep slope on the East face and a smooth slope on the West face. These are identified as fault scarps, which have a free face to ESE with maximum heights of 8 m that decrease to ESE down to 0.5 m. In the fault scarps, the values of the slope measured in the profile exceeded 9°, reaching values of up to 45° (Fig. 3a). In the case of the river profiles the topographic height also decreases towards

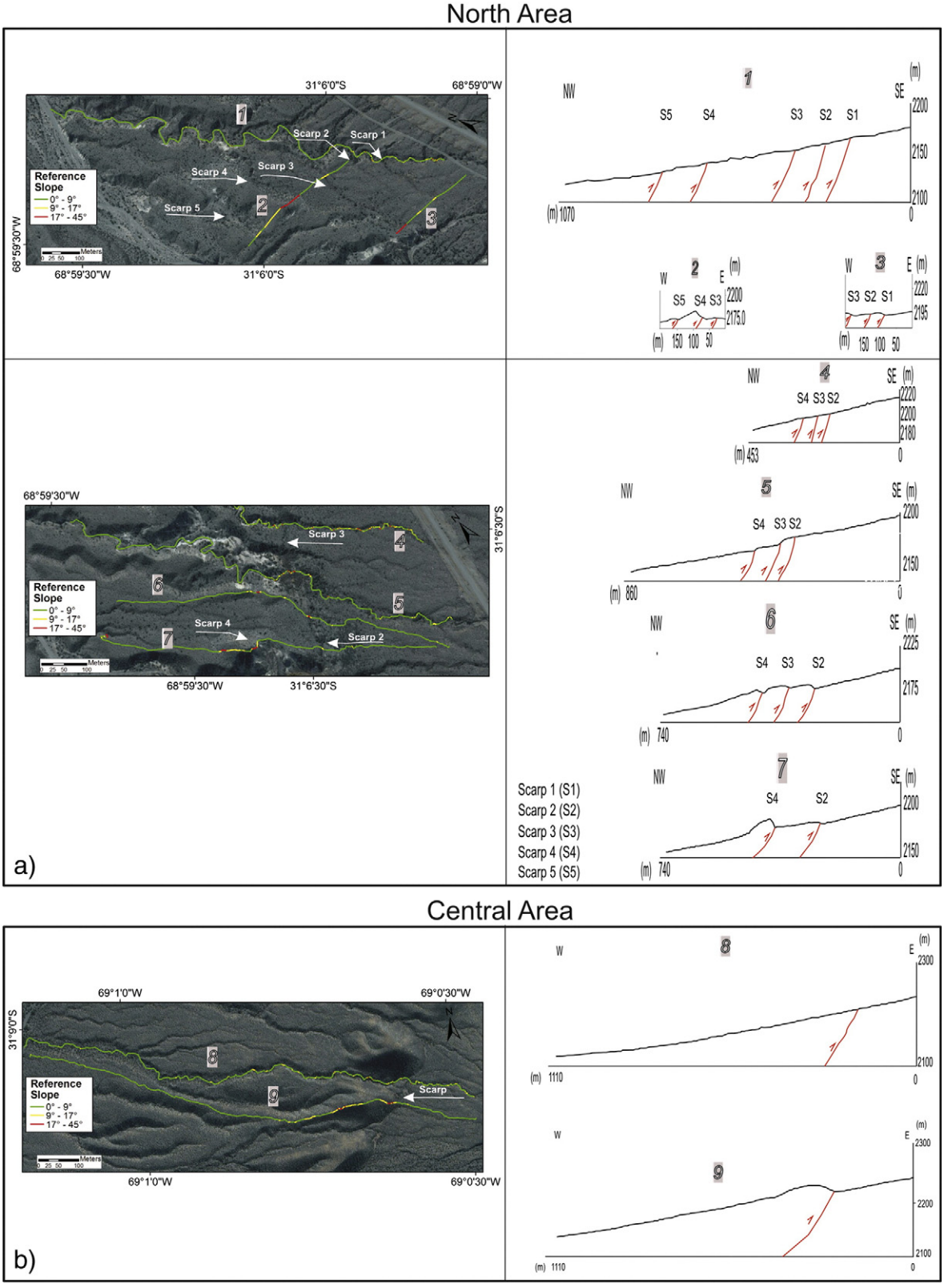

Fig. 3. High-resolution topographic profiles perpendicular to the LCFS trace (north and central sections) along small temporary streams (1, 4, 5 and 8) and interfluves (2, 3, 6, 7 and 9).

WNW. The topographic profiles of the rivers present a linear trend, and small knickpoints are observed. In this case, the observed disruptions correspond to counterslope steps and laterally coincide with fault scarps; however, this pattern was more conspicuous in profile 5, where there are waterfalls. The slope in the disruption segments reaches values of approximately 16°. Topographic anomalies in the interfluves are more obvious than along river profiles, which may result from fluvial erosion reducing the morphological pattern. Taking into account the height of the higher scarp, it was possible to calculate a net maximum vertical displacement of 15 m for a fault in this area during

the Quaternary. Furthermore, these topographic profiles along interfluves helped to obtain the shortening of the western piedmont of sierra de La Cantera, which is around 4%.

In the central portion (Fig. 3b) the profile of the interfluve shows that topographic height decreases to the west and a remarkable hunch can be observed with an asymmetric shape, having an abrupt slope on the east face and smooth slope to the west. The observed hunch is a fault scarp with a free face to the east, which has a height of 13 m (Fig. 2b) that was generated by a Quaternary fault and modifies the local slope to values between 9° and 15°, although sometimes it exceeds 15°. The net maximum vertical displacement produced by the fault during Quaternary in the area was 16 m, and the shortening around 3%. As in the north (Fig. 3a), it is not easy to recognize topographic changes along the river. Furthermore, when the gradient was calculated for the river profiles, several knickpoints were identified but could not be related directly to fault activity. Finally, in the north portion, morphological markers are more abundant in the interfluve and rivers, like multiple counterslope scarps (Fig. 1c), incised and sinuous rivers in the hanging block, sag ponds (Figs. 1c, 4), alluvial terraces entirely located in the hanging block and aligned springs (Figs. 1c; 5a, b), whereas in the South, although there are few, fault scarps exhibit the highest topographic height.

The smoothing of topographic anomalies observed in rivers has been related to the ability of fluvial dynamics to adapt to slope variations. Small temporary rivers that drain the western piedmont of the Sierra de La Cantera often reflect subtle topographic modifications (Fig. 5a). Perucca et al. (2014a) analyzed several river anomalies related to the northern segment of the LCFS and described the relationships between stream sinuosity and slope in these rivers, observing that the most sinuous channels have lower slopes and are located on the hanging wall of the fault (Fig. 5a). Morphometric analysis of the scarps indicates that Holocene tectonics have played a major role in controlling the drainage pattern in the piedmont, leading the rivers to adjust to these slope variations.

Perucca et al. (2014b) investigated the deformational style variations along the La Cantera Fault System, describing a series of landforms typical of active compressive tectonics. These authors noted flexural counterslope fault scarps, with heights ranging from 0.3 m to 8 m, corresponding to vertical displacements accumulated during the Late Pleistocene–Holocene. The highest elevations were recognized in the central section of the fault. The minimum displacement measured on the fault plane in natural trenches varied between 0.50 m and 1.80 m. Both erosional and depositional terraces are present; only three levels of unpaired terraces are identified in the hanging block, on the right bank of streams that cross the fault (Fig. 5a, b).

The drainage pattern anomalies in the area reflect subtle changes of topography that have been induced by active tectonics, such as river diversion, beheaded and captured streams, changes in the incision depth, sinuosity and river gradient along streams, wind gaps, sag ponds, tectonic gutters and broom-shaped river patterns (Perucca et al., 2014a, b). Therefore, an analysis of the drainage pattern is an important tool in the study of tectonic activity in thrust fault systems because they are highly sensitive to vertical tectonic uplifts related to folds and thrusts (Audemard, 1999, 2003; Ollarves et al., 2007).

Along the entire trace of the LCFS, small sag ponds and springs directly related to fault trace were located (Figs. 4a, 5a). A sequence of silt–mud beds was deposited in a small sag pond along the La Cantera Fault Scarp during the late Holocene (Fig. 4b). A sample (CA1) collected in one of these charcoal detritus beds was radiocarbon dated at Cal 2600 ± 30 years BP, establishing that the fault has been active within the recent geologic past controlling piedmont drainage pattern (Table 1). Fig. 4 (c and d) shows a counterslope scarp, ranging from 0.30 cm to 1.70 cm of height, that deflected a stream when it met the scarp. This 0.30 cm scarp could be related to that mentioned by

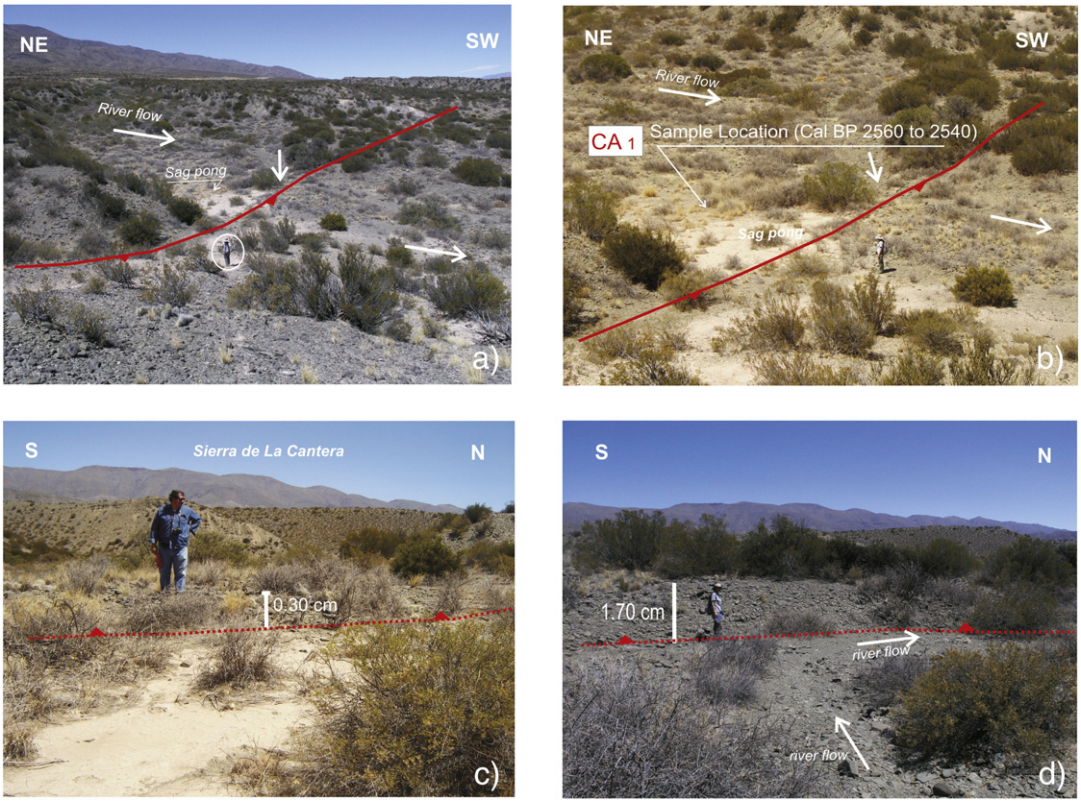

Fig. 4. a) View of a tectonic depression filled with fine sediments (sag pond) and a ~30 cm counterslope scarp that diverts a recent stream. Location of sample CA1 is also indicated; b) view to the west showing the very recent scarp, c) detail of the sagpond and little scarp facing to the east and d) view to the west of the counterslope scarp and river flow deflection.

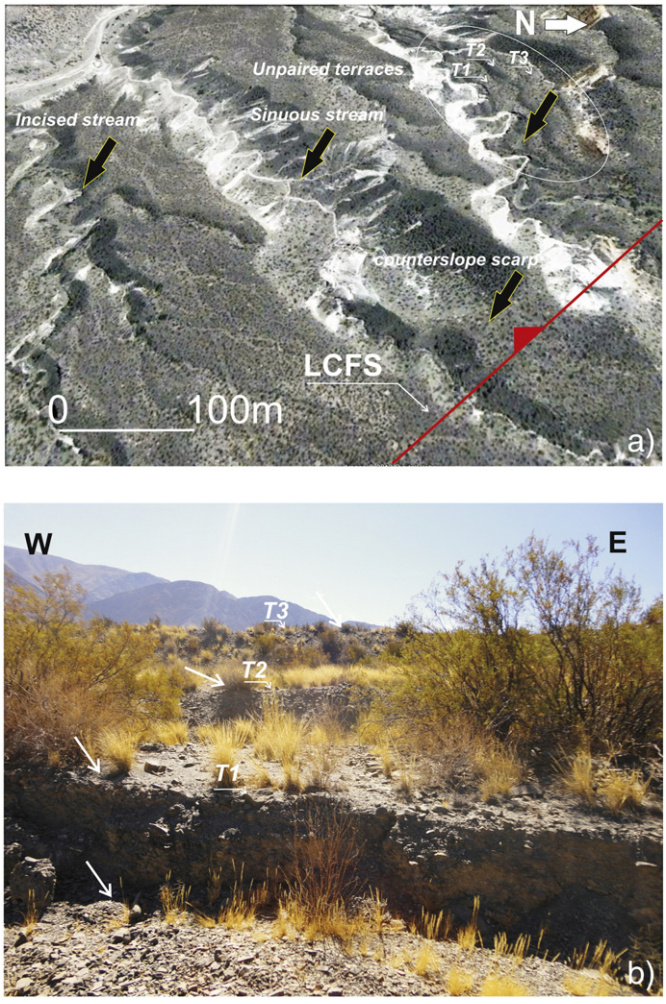

Fig. 5. a) Google Earth oblique view showing the adjustment of rivers (black arrows) to the fault scarp changing in some cases from straight to sinuous or/and increasing density of channels. Three unpaired terraces (pointed with white arrows) were recognized only in the northern bank of the streams, b) unpaired terraces were only identified in the northern margin of streams, in the hanging block of LCFS.

Mingorance (1998), which was originated during the 1924 earthquake rupture.

4.2. Kinematics and chronology of faulting events

Fault exposures have been analyzed along the LCFS to assess their kinematics and other characteristics. Data were gathered from metric scale outcrops located along river cuts. In all of the natural trenches, the east-vergent faults trend between 150° to 190° and dip 10° to 40° W.

Perucca et al. (2014b) studied three natural exposures along the entire fault trace and observed that the faults cut Holocene deposits in the north, whereas to the south, they affect older levels of possible Pleistocene deposits. Holocene deposits are not deformed at this site, behaving as blind thrusts. They recognize two colluvial wedges, implying the occurrence of two seismic events during the Holocene–Pleistocene.

Geomorphological features described in this work, together with four natural exposures analyzed and dated using the AMS method, indicate Holocene tectonic activity on the LCFS, which can be traced to mid- to late-Holocene soil levels (4580 ± 50 BP to 1576 to 1423 Cal years BP) and early to mid-Holocene alluvial terraces (11,962 to 11,615 Cal years BP to 4865 to 4830 Cal years BP).

In Trench 1, located in the North section of the LCFS, three-hundred meters west of route 148 (Fig. 1c), a low temperature spring can be directly related to the fault trace (31° 6′S–68° 59′W). The oldest exposed unit (Unit Q2) corresponds to angular-to-subangular gravel-dominated alluvial deposits of unknown base and to a maximum exposed thickness of 1 m. Spring silt–mud deposits lay over alluvial gravels to a Q2 level. The ^{14}C dates for these orange-yellowish sediments indicate late-Holocene ages (Sample CA 2, 1576 to 1423 Cal years BP) (Table 1). An east-verging thrust cuts across the alluvial level Q2 as well as spring deposits, striking N17° and dipping 30° W. The whole sequence is capped by a modern incipient soil (Fig. 6a).

In Trench 2, 200 m south of trench 1 (31° 6.7′S–68° 59.3′W), another natural exposure allows observation of deformation produced by the fault (Fig. 1c). Surface expression of the main fault here is represented by a 1 m scarp, but there is no noticeable surface rupture expression at the site. The trench stratigraphy is composed of five main units labeled Ne through Ms in Fig. 6b. The oldest exposed unit (Ne) corresponds to pink Neogene sandstones and siltstones of unknown base and a maximum exposed thickness of 0.70 m. These rocks are partly overlain by angular-to-subangular gravel-dominated alluvial deposits (Q2). In the hanging block, Ne and Q2 are partially covered by a beige incipient paleosoil horizon (S1) and by a light-brownish paleosoil horizon (S2). The uppermost unit (Ms) corresponds to a modern brownish soil horizon. The boundaries among these beds are not very well defined. The fault, trending 300–320° and dipping 34°–36° W, affects the Neogene unit (Ne), the alluvial deposits (Q2) and the two soil layers (S1 and S2). The fault slip has caused clast rotation and an imbricate fabric subparallel to the fault plane but the fault trace has no noticeable surface expression at the trench site (Figs. 1c, 6b). Millán and Perucca (2011) recognized two colluvial wedges in the footwall, inferring two events during the Holocene on that portion of the fault.

As was previously pointed out by Deng and Zhang (2000), a reverse fault may rupture repeatedly and each offset event could be associated with a colluvial wedge and so, they can be used to recognize earthquake events. In spite of a foot slope colluvium origin could not be dismissed in natural exposures analyzed along the La Cantera Fault System, we consider these chaotic deposits as colluvial wedges derived from erosion of the upthrown block. All of them have angular and unsorted pebbles and sands that are in-situ deposited, the grain sizes decrease away from the fault scarp and the contact between the fault and the unsorted deposits is the plane of the thrust.

The oldest fault event recorded in the trench is constrained by units Ne and S1, and, according to the radiocarbon ages of the paleosoil S1, it might have taken place after 4580 ± 50 BP (Sample CA3 in this work). When another seismic event would happen, it will produce a new fault scarp and generate space enough for the development of a second colluvial wedge (Millán and Perucca, 2011).

Table 1
Radiocarbon ages for faults discussed in text.

Sample data	Method	Material	Measured radiocarbon age	$^{13}C/^{12}C$ ratio	Conventional radiocarbon age	2σ calibrated age
Beta-392411 CA1	AMS	Organic detritus	2520 ± 30 BP	−20.4‰	2600 ± 30 BP	Cal BP 2750 to 2700 Cal BP 2630 to 2620 Cal BP 2560 to 2540
Beta-392414 CA2	AMS	Organic detritus	1600 ± 30 BP	−21.6‰	1660 ± 30 BP	Cal BP 1576 to 1423
Beta-392410 CA4	AMS	Organic detritus	1720 ± 30 BP	−19.9‰	1800 ± 30 BP	Cal BP 1735 to 1590
Beta-392412 CA5	AMS	Organic detritus	10,160 ± 40 BP	−23.8‰	10,180 ± 40 BP	Cal BP 11,962 to 11,615
Beta-392413 CA6	AMS	Charcoal detritus	4220 ± 30 BP	−19.2‰	4320 ± 30 BP	Cal BP 4865 to 4830

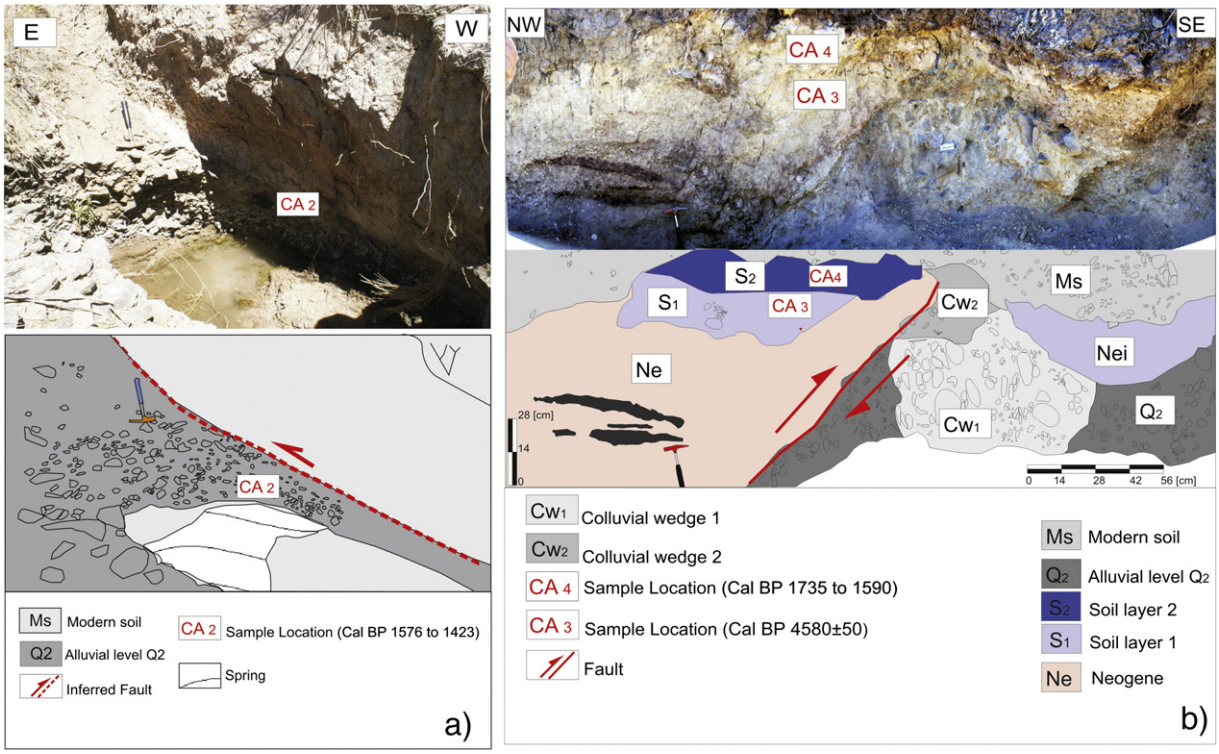

Fig. 6. a) Trench 1 and a view of the upper part of the south wall of La Cantera Spring with the location of sample CA2; b) natural trench 2, where Neogene rocks and mid–late Holocene soils override fluvial deposits on the north trace of the La Cantera thrust (modified from Millán and Perucca, 2011). The location of samples (CA3 and CA4) on the hanging wall and two colluvial wedges in the footwall are indicated. The fault trends 304° to 320° and dips 34° W.

In this research, AMS (accelerator mass spectrometry) ^{14}C measurements were used (Table 1). Upper soil horizon (S2) ^{14}C dates yield late-Holocene ages (Sample CA4, 1735 to 1590 Cal years BP). Therefore, the last identified seismic event horizon would have taken place after the deposition of unit S2. The uppermost soil layer (Ms) seems unaffected by the fault (Fig. 6b).

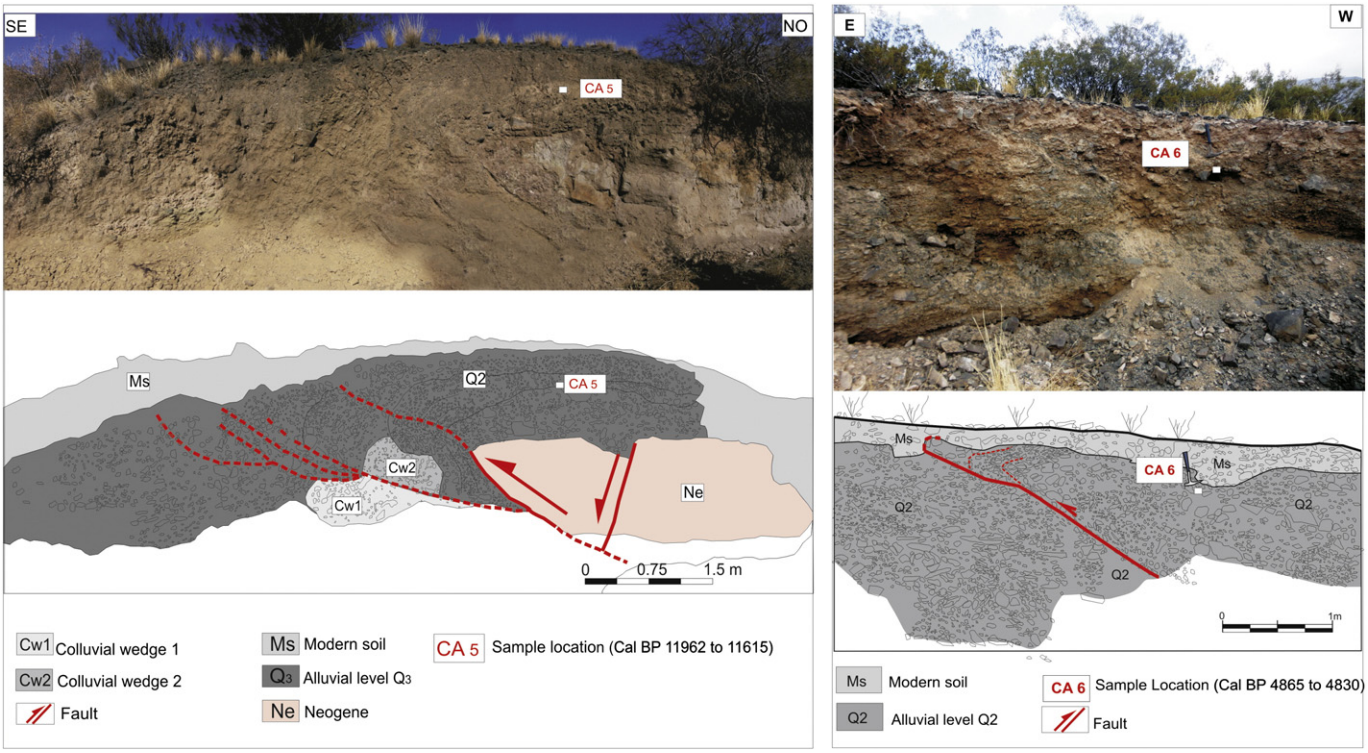

Fig. 7. a) Trench 3, showing an east-verging thrust where Oligocene–Miocene sedimentary rocks override the Quaternary alluvial gravels, as well as the location of sample CA5. The fault plane strikes N17° and dips 50° NW (modified from Perucca et al., 2014a,b). Thrusting does not show surface rupture; b) natural exposure of trench 4, showing a fault propagation fault in alluvial gravels of mid-Holocene age, as well as the location of Sample CA6.

In Trench 3 (a natural trench), which is located in the central segment of the LCFS, 1.5 km east of the road (31° 8′ 53″S–69° 0′ 22″W) (Fig. 1c) exposes 3.5 m of Q2 alluvial sequence, comprising several clast-supported tabular beds in its lower half and is rich in angular pebbles in a sandy matrix. This package rests, non-conforming, on top of reddish late Oligocene to late Miocene sedimentary rocks and dips few degrees (5–10°) to the west. An east-verging thrust puts Oligocene–Miocene sedimentary rocks over Quaternary alluvial gravels. The fault plane strikes N17° and dips 50° NW. It does not cut the surface, but a gentle flexure of the terrace top coincides with the brittle deformation displayed in the outcrop (Fig. 7a). A sample collected in the Q2 level yielded ^{14}C Late Pleistocene–Early Holocene ages (Sample CA5, 11,962 to 11,615 Cal years BP) (Table 1).

The thrust fault cuts essentially through angular-to-subangular gravel-dominated deposits containing sparse large boulders (<30 cm). The lower and middle parts of the gravel terrace are thrust faulted towards the east, whereas the younger upper part is only warped and presents itself as a gentle flexure at the terrace surface. The presence of two colluvial wedges deriving from the tectonic scarp, a coarser basal one and a more clayey one above, would also suggest the occurrence of two Holocene events on this fault (Fig. 7a).

In trench 4 this exposure is located approximately 340 m south of trench 3 (31° 9′4.2″S–69° 0′26.2″W) (Fig. 1c). The thrust affects a ~3 m high fill terrace. The exposed trench section reveals a very low-angle fault affecting the Q2 unit. The fault plane trends 330° to 3° and dips between 26° W near the surface to 56° W at depth (Fig. 7b). The terrace gravels are a sub-angular to angular, poorly sorted cobble–pebble sequence (Q2 level). Internal folding is well represented by the preferred orientation of the gravel clasts.

The faulting displaces the gravels of Units Q2 and modern soil (Ms unit) seems to be folded too, although it is not clear. Unit Q2 exhibits prominent folding along a low-angle fault. The folding of this unit along the fault suggests that part of the slip has also been consumed in folding. Besides, Unit Q2 shows more cumulated slip than the uppermost layers thus indicating than more than one event appears to be recorded by this Unit. Radiocarbon dating of detrital charcoal from unit Q2, collected from the hanging wall in the overthrusted block, yielded a Mid Holocene age (Sample CA6, 4865 to 4830 Cal years BP) (Table 1). So that it would indicate a last seismic event younger than the deposition of this sampled layer.

5. Discussion and conclusions

Central Precordillera has a mountainous relief characterized by N–S trending linear ranges and basins. Thrust faults bound Paleozoic ranges and narrow linear valleys filled with Neogene to Quaternary continental sediments (Jordan et al., 1993; von Gosen, 1992). Central Precordillera has been described as a thin-skinned thrust-and-fold belt due to Neogene crustal shortening on west dipping, imbricated structures that root down to a 10–15 km deep main *décollement* (Allmendinger et al., 1990; Jordan et al., 1993; Ramos and Cristallini, 1995; von Gosen, 1992).

The La Cantera Fault System, located in the intermontane valley between the Sierra de La Cantera and the Sierra de La Invernada, in Central Precordillera, provides remarkable geomorphological evidence of Quaternary tectonic activity. Nine topographic profiles along the river and interfluves were carried out on the Western piedmont of the Sierra de la Cantera. The profiles were grouped into two areas (North and Central sections). The topographic profiles of the interfluves exhibited asymmetric fault scarps with free faces to the East-Southeast. In the North portion, five parallel scarps were identified with heights from 0.5 m to 8 m. A net maximum displacement of 15 m and shortening of 4% related to the Quaternary identified scarps was obtained. On the other hand, in the South section only one scarp was recognized, with a height of 13 m (Fig. 2b) and the net displacement was around 16 m with a shortening of 3%. The topographic profiles of the rivers exhibited small steps in the talweg, and a small waterfall was identified in profile 5. These disruptions in both types of profile (river and interfluve) are associated with Quaternary fault activity. The geographic distribution of topographic anomalies, which are more profuse in the North than in the Central section, are the morphological response to a higher quantity of fault traces in the North, whereas they are restricted to one fault trace in the South.

Recent paleoseismic investigations in the LCFS reveal preliminary evidence of at least four earthquakes during the past 11,000 years in coincidence with results obtained by Mingorance (1998). The observed deformation of the alluvial Q2 terrace with two colluvial wedges in the Central segment of the LCFS (11,962 to 11,615 Cal years BP, trench 3) suggests that at least two, pre-1924 paleoearthquakes are preserved in these alluvial deposits. In the other two trenches located in the Northern and Central portion of the LCFS, the fault affects the poorly-developed soil with a mid-Holocene age (4580 ± 50 Cal years BP in trench 1); furthermore, an organic detritus from a Q2 terrace unit collected from the hanging wall in the overthrusted block (Central portion of the LCFS) also yielded a Mid Holocene age (4865 to 4830 Cal years BP, in trench 4).

A sample collected in a sag pond associated with a 0.30 cm counterslope scarp was radiocarbon dated at Cal 2600 ± 30 years BP, indicating that the fault was active during the late Holocene. Mingorance (1998) pointed out that the 1924 earthquake (Ms = 6.0) did rupture on the La Cantera Fault System, creating a 0.30 cm scarp, and that at least three prehistoric surface rupture events can be recognized based on fault scarp analysis. Therefore, the 0.30 cm scarp related to the sampled sag pond could be associated to the last historical event mentioned by Mingorance (1998). On the other hand, an upper soil horizon (S2) affected by the fault in trench 2 was ^{14}C dated, yielding late-Holocene ages, similar to the age obtained in the spring deposits at trench 1. This could indicate that a penultimate earthquake occurred when the soil and spring deposits were at the surface, between 1700 and 1400 Cal years BP.

Our results indicate that the seismogenic zone accommodates a recurrent interval of at least 2000 ± 500 years. Even though the age constraints provided by our study are not good enough to fully test this assumption, recurrence of multiple events (at least three earthquakes) during the last 11,000 years is very significant for seismic hazard assessment because presently, no sufficient paleoseismic data in this region of Central Precordillera is available. This information will play an important role in evaluating seismic hazards in this area.

Acknowledgements

The authors acknowledge funding from PIP 0799-2010 (CONICET), PICTO AGENCIA — UNSJ 09/13-Préstamo BID and CAPES-Mincyt Br1201 for support of this research. We thank two anonymous reviewers and tectonophysics editor Kelin Wang for constructive criticism, which greatly improved our study.

References

Allmendinger, R., Figueroa, D., Zinder, E., Beer, J., Mpodozis, C., Isacks, B.L., 1990. Foreland shortening and crustal balancing in the Andes at 30° latitude. Tectonics 9, 789–809.
Alvarado, P., Beck, S., 2006. Source characterization of the San Juan (Argentina) crustal earthquakes of 15 January 1944 (Mw 7.0) and 11 June 1952 (Mw 6.8). Earth Planet. Sci. Lett. 243, 615–631.
Anderson, M., Alvarado, P., Zandt, G., Beck, S.L., 2007. Geometry and brittle deformation of the subducting Nazca Plate, central Chile and Argentina. Geophys. J. Int. 171, 419–434.
Audemard, F., 1999. Morpho-structural expression of active thrust fault systems in the Humid Tropical Foothills of Colombia and Venezuela. Z. Geomorphol. 118, 1–18.
Audemard, F., 2003. Geomorphic and geologic evidence of ongoing uplift and deformation in the Mérida Andes, Venezuela. Quat. Int. 101-102C, 43–65.
Barazangi, M., Isacks, B.L., 1976. Spatial distribution of earthquakes and subduction of the Nazca plate beneath South America. Geology 4, 686–692.
Costa, C., Audemard, F., Bezerra, H., Lavenu, A., Machette, M., Paris, G., 2006. An overview of the main Quaternary deformation of South America. Rev. Asoc. Geol. Argent. 61, 461–479.

Cristallini, E.O., 1998. Introducción a las fajas plegadas y corridas. I. Las fajas plegadas y corridas (Unpublished), 4–92.
Cristallini, E.O., Ramos, V.A., 2000. Thick-skinned and thin-skinned thrusting in the La Ramada fold and thrust belt: crustal evolution of the High Andes of San Juan, Argentina (32° SL). Tectonophysics 317, 205–235.
Deng, Q., Zhang, P., 2000. Colluvial wedges associated with pre-historical reverse faulting paleoearthquakes. Chin. Sci. Bull. 45, 1598–1604.
Gutiérrez Elorza, M., 2008. Geomorfología. Pearson Educación S.A. Madrid, España (920 pp.).
Holbrook, J., Schumm, S.A., 1999. Geomorphic and sedimentary response of rivers to tectonic deformation: a brief review and critique of a tool for recognizing subtle epeirogenic deformation in modern and ancient settings. Tectonophysics 305, 287–306.
Jordan, T.E., Allmendinger, R.W., Damati, J.F., Drake, R.E., 1993. Chronology of motion in a complete thrust belt: the Precordillera, 30–31°S, Andes Mountains. J. Geol. 101, 137–158.
Kendrick, E., Bevis, M., Smalley, R.J., Brooks, B., Vargas, R.B., Lauría, E., Fortes, L.P., 2003. The Nazca–South America Euler vector and its rate of change. J. S. Am. Earth Sci. 16, 125–131.
Levina, M., Horton, B., Fuentes, F., Stockli, D., 2014. Cenozoic sedimentation and exhumation of the foreland basin system preserved in the Precordillera thrust belt (31–32°S), southern central Andes, Argentina. Tectonics 33, 1659–1680.
Martinod, J., Husson, L., Roperch, P., Guillaume, B., Espurt, N., 2010. Horizontal subduction zones, convergence velocity and the building of the Andes. Earth Planet. Sci. Lett. 299, 299–309.
McCalpin, J.P., 2009. Paleoseismology. International Geophysics Series 2nd ed. Academic Press, London (613 pp.).
Milana, J.P., Cevallos, M., Zavattieri, A., Prampano, M., y Papu, H., 1993. La secuencia terciaria de Pachaco: sedimentológica, edad, correlaciones y significado paleogeográfico. 12° Congreso Geológico Argentino and 2° Congreso de Exploración de Hidrocarburos 1, pp. 226–234.
Millán, J.L., Perucca, L., 2011. Análisis neotectónico del extremo norte del sobrecorrimiento La Cantera, provincia de San Juan, Argentina. Rev. Mex. Cienc. Geol. 18, 337–348.
Mingorance, F., 1998. Evidencias de paleoterremotos en la falla activa La Cantera-Cinturón de empuje de la Precordillera, San Juan, Argentina. 10° Congreso Latinoamericano de Geología 2, pp. 161–166.
Morley, C.K., 1988. Out of sequence thrusts. Tectonics 7, 539–561.
Ollarves, R., Audemard, F., Lopez, M.C., 2007. Morphotectonic criteria for the identification of active blind thrust faulting in alluvial environments: case studies from Venezuela and Colombia. In: Latrubesse, E. (Ed.), Tropical Geomorphology. Zeitschrift für Geomorphologie, Supplementbände. Gebr. Borntraeger Verlagsbuchhandlung, Science Publishers, Stuttgart, pp. 81–103.
Pardo, M., Comte, D., Monfret, T., 2002. Seismotectonic and stress distribution in the central Chile subduction zone. J. S. Am. Earth Sci. 15, 11–22.
Pardo-Casas, F., Molnar, F., 1987. Relative motion of the Nazca (Farallon) and South American plates from Late Cretaceous time. Tectonics 6, 233–248.
Perucca, L., Pérez, M., Navarro, C., 2006. Fenómenos de licuefacción asociados a terremotos históricos. Su análisis en la evaluación del peligro sísmico en la Argentina 61. Revista de la Asociación Geológica Argentina, pp. 567–578.
Perucca, L., Rothis, M., Vargas, H., 2014a. Morphotectonic and neotectonic control on river pattern in the Sierra de la Cantera piedmont, Central Precordillera, province of San Juan, Argentina. Geomorphology 204, 673–682.
Perucca, L., Onorato, M., Millán, J., Bustos, A., Vargas, H., 2014b. Variación del estilo de deformación a lo largo del Sistema de falla La Cantera, Precordillera Central, San Juan, Argentina. Rev. Soc. Geol. Esp. 27, 69–79.
Pilger, R.H., 1981. Plate reconstructions, aseismic ridges, and low angle subduction beneath the Andes. Geol. Soc. Am. Bull. 92, 448–456.
Ramos, V.A., 1988. The tectonics of the Central Andes; 30° to 33°S latitude. In: Clark, S., Burchfiel, C. (Eds.), Processes in Continental Lithospheric Deformation. Geological Society of America, Special Paper 218, pp. 31–54.
Ramos, V.A., 1999. Plate tectonic setting of the Andean Cordillera. Episodes 22, 183–190.
Ramos, V.A., Cristallini, E., 1995. Perfil estructural de la Precordillera a lo largo del Río San Juan. Andean Thrust Tectonics Symposium, Field Guide, San Juan, Argentina, pp. 1–42.
Ramos, V.A., Vujovich, G.I., 2000. Hoja Geológica 3169-IV, San Juan, Provincia de San Juan. Boletín 243, Subsecretaría de Minería Nación, Servicio Geológico Minero Argentino (82 pp., Buenos Aires).
Ramos, V.A., Cegarra, M.I., Lo Forte, G., y Comíngues, A., 1997. El frente orogénico de la sierra de Pedernal (San Juan, Argentina): su migración a través de los depósitos sinorogénicos. Actas 8° Congreso Geológico Chileno 3, pp. 1709–1713 (Chile).
Ramos, V.A., Cristallini, E.O., Pérez, D., 2002. The Pampean flat-slab of the Central Andes. J. S. Am. Earth Sci. 15, 59–78.
Rosenbaum, G., Mo, W., 2011. Tectonic and magmatic responses to the subduction of high bathymetric relief. Gondwana Res. 19, 571–582.
Siame, L., Bellier, O., Sebrier, M., 2006. Active tectonics in the Argentine Precordillera and western Sierras Pampeanas. Rev. Asoc. Geol. Argent. 61, 604–619.
Smalley Jr., R., Isacks, B.L., 1990. Seismotectonics of thin and thick-skinned deformation in the Andean foreland from local network data: evidence for a seismogenic lower crust. J. Geophys. Res. 95, 12487–112498.
Smalley Jr., R., Pujol, J., Regnier, M., Chiu, J.M., Chatelain, J.L., Isacks, B.L., Araujo, M., Puebla, N., 1993. Basement seismicity beneath the Andean Precordillera thin-skinned thrust belt and implications for crustal and lithospheric behavior. Tectonics 12, 63–76.
Vigny, C., Rudloff, A., Ruegg, J.C., Madariaga, R., Campos, J., Alvarez, M., 2009. Upper plate deformation measured by GPS in the Coquimbo Gap, Chile. PEPI 175, 86–95.
Von Gosen, W., 1992. Structural evolution of the Argentine Precordillera: the Rio San Juan section. J. Struct. Geol. 14, 643–667.
Whitney, R., Bastías, H., 1984. The Tigre fault of the San Juan Province, Argentina—the late Quaternary boundary of the Andes uplift. Geol. Soc. Am. Prog. Abstr. 16, 6–693.
Yáñez, G., Ranero, C., von Huene, R., Díaz, J., 2001. Magnetic anomaly interpretation across the southern Central Andes (32°–34° S): the role of the Juan Fernandez Ridge in the late Tertiary evolution of the margin. J. Geophys. Res. Solid Earth 106, 6325–6345.